CRLX101 nanoparticles localize in human tumors and not in adjacent, nonneoplastic tissue after intravenous dosing

Andrew J. Clark[a], Devin T. Wiley[a], Jonathan E. Zuckerman[a,b], Paul Webster[c], Joseph Chao[d], James Lin[e], Yun Yen[f,1], and Mark E. Davis[a,1]

[a]Division of Chemistry and Chemical Engineering, California Institute of Technology, Pasadena, CA 91125; [b]Department of Pathology and Laboratory Medicine, University of California, Los Angeles, CA 90095; [c]Oak Crest Institute of Science, Pasadena, CA 91107; [d]Department of Medical Oncology, City of Hope Comprehensive Cancer Center, Duarte, CA 91010, [e]Division of Gastroenterology, City of Hope Comprehensive Cancer Center, Duarte, CA 91010; and [f]Graduate Institute for Cancer Biology and Drug Discovery, Taipei Medical University, Taipei 11031, Taiwan

Contributed by Mark E. Davis, February 23, 2016 (sent for review February 3, 2016; reviewed by Omid Farokhzad and David V. Schaffer)

Nanoparticle-based therapeutics are being used to treat patients with solid tumors. Whereas nanoparticles have been shown to preferentially accumulate in solid tumors of animal models, there is little evidence to prove that intact nanoparticles localize to solid tumors of humans when systemically administered. Here, tumor and adjacent, nonneoplastic tissue biopsies are obtained through endoscopic capture from patients with gastric, gastroesophageal, or esophageal cancer who are administered the nanoparticle CRLX101. Both the pre- and postdosing tissue samples adjacent to tumors show no definitive evidence of either the nanoparticle or its drug payload (camptothecin, CPT) contained within the nanoparticle. Similar results are obtained from the predosing tumor samples. However, in nine of nine patients that were evaluated, CPT is detected in the tumor tissue collected 24–48 h after CRLX101 administration. For five of these patients, evidence of the intact deposition of CRLX101 nanoparticles in the tumor tissue is obtained. Indications of CPT pharmacodynamics from tumor biomarkers such as carbonic anhydrase IX and topoisomerase I by immunohistochemistry show clear evidence of biological activity from the delivered CPT in the posttreatment tumors.

nanomedicine | clinical trial | gastric cancer | tumor targeting | nanoparticles

Nanoparticle-based experimental therapeutics are being used to deliver a variety of different drug molecules to patients with solid tumors (1). Nanoparticle delivery seeks to improve pharmacokinetic (PK) properties (e.g., enhanced solubility of the drug, increased circulation times), alter biodistribution of the drug molecules to have low amounts of drugs in nontarget tissues and increased amounts in tumors, and enhance pharmacodynamics (PD) (e.g., tunable release of the drug at the site of action in the tumor) to produce enhanced efficacy while simultaneously reducing side effects (and most importantly, introducing no new side effects due to the nanoparticle) in patients. These properties can: (*i*) enable drug combinations formerly prohibited by toxicity limits, (*ii*) enable new classes of drug delivery [for example, short interfering RNAs (siRNAs)], and (*iii*) provide cell-specific targeting within a tumor.

Delivery of drugs to solid tumors using nanoparticle technology relies on the enhanced permeability and retention (EPR) effect. The mechanistic data regarding the EPR effect come from animal models, primarily xenografted human tumors in mice. Because these xenografted tumors poorly recapitulate the architecture of true human tumors, there is skepticism about whether or not intact nanoparticles can localize in human tumors. Radiolabeled liposomes have been used to assess tumor accumulation in humans (2, 3). In those studies, the amounts of radioactivity accumulated in tumors did correlate with the number of microvessels measured from nine patient biopsies (3). Increased microvessel density may be an indication of increasing potential for the EPR effect. Also, Davis et al. demonstrated dose-dependent deposition of the CALAA-01 polymer–siRNA nanoparticle system in human s.c. melanoma metastases using a stain specific for the nanoparticle (4); Eliasof et al. showed the presence of the camptothecin (CPT) component of CRXL101 in a single human gastric tumor biopsy (5); and Weiss et al. provided a single biopsy showing CRLX101 and CPT in a human breast cancer (6). Thus, there remains a need for further evidence of intact nanoparticle localization in solid, human tumors when they are systemically administered to cancer patients.

Here, we use fluorescence microscopy to demonstrate the presence of an intact polymer-drug nanoparticle (CRLX101) in human gastric tumors that have been obtained from endoscopic capture before, and 24–48 h after, dosing. Adjacent, nonneoplastic tissues are also obtained to assist in determining the specificity for tumor localization. Further, immunohistochemistry (IHC) was used to label various biomarkers within the tumor tissue to better understand the pharmacodynamics effect of CRLX101 on solid human tumors.

CRLX101 is a nanoparticle consisting of a cyclodextrin-containing polymer conjugate of CPT. The individual polymer strands self-assemble into nanoparticles (approximately five strands) of

Significance

Nanoparticle-based therapeutics rely on the enhanced permeability and retention effect to localize in solid tumors and not healthy tissue. These phenomena are rationalized from animal models of human disease. Since these models poorly represent human tumors, there is a need to obtain information from humans to better understand how nanoparticle-based therapeutics perform in humans. Here, we collected tumor and nonneoplastic tissue biopsies from cancer patients who have been administered CRLX101 and show that the intact nanoparticles localize in human tumors and not in adjacent tissues. Sufficient concentrations reach the tumors to cause down-regulation of topoisomerase I and carbonic anhydrase IX. These results will aid in better understanding how nanoparticle therapeutics function in humans and how to better design future therapeutics.

Author contributions: A.J.C., D.T.W., J.E.Z., P.W., J.C., Y.Y., and M.E.D. designed research; A.J.C., D.T.W., J.E.Z., P.W., J.C., and J.L. performed research; A.J.C., D.T.W., J.E.Z., P.W., J.C., Y.Y., and M.E.D. analyzed data; and A.J.C., J.E.Z., Y.Y., and M.E.D. wrote the paper.

Reviewers: O.F., Harvard Medical School; and D.V.S., University of California, Berkeley.

Conflict of interest statement: M.E.D. is a consultant to Cerulean Pharma Inc. and owns stock in the company.

Freely available online through the PNAS open access option.

[1]To whom correspondence may be addressed. Email: mdavis@cheme.caltech.edu or yyen@tmu.edu.tw.

This article contains supporting information online at www.pnas.org/lookup/suppl/doi:10.1073/pnas.1603018113/-/DCSupplemental.

~20- to 30-nm diameter and 10 wt% CPT by multiple, interstrand, inclusion complex formation between cyclodextrin and the CPT molecules (Fig. 1*A*). CRLX101 is currently in a number of human cancer phase II trials (early results from some of the phase I/II trials are available) (6, 7). Here, a clinical trial was performed at and sponsored by the City of Hope Comprehensive Cancer Center (ClinicalTrials.gov identifier: NCT01612546). CRLX101 was supplied by Cerulean Pharma Inc. The primary endpoint of this study was to test the hypothesis that intact CRLX101 nanoparticles localize in primary human tumors and not adjacent, nonneoplastic tissue after i.v. administration. The results presented here show that CRLX101 does localize in tumor tissue and not the nonneoplastic tissue leading to the expected pharmacodynamics effect.

Results

Trial Design and Tissue Biopsies. Patients with progression on at least one prior line of systemic therapy were enrolled in a pilot study to assess CRLX101 activity in gastric, esophageal, or gastroesophageal adenocarcinoma or squamous cell carcinoma (Fig. 1*B*). Patients consented to have endoscopic-assisted biopsies of both their primary tumor and nonneoplastic, adjacent tissue before, and 24–48 h after, the first dose of CRLX101. The first dose of CRLX101 for all patients was given at the recommended phase II dosing of 15 mg/m^2. Three individual samples of both tumor and nonneoplastic tissue were acquired and divided in the following ways: (*i*) frozen in optimized cutting temperature compound (Tissue-Tek OCT) for fluorescence microcopy studies, (*ii*) fixed in 10% formalin for antibody staining, or (*iii*) placed in formalin for standard histology. A total of 10 patients consented for this study, of which 9/10 had histologically confirmed tumor tissue present in both pre- and post-CRLX101 treatment biopsies.

Detection of CRLX101 Fluorescence in Human Gastric Tumors. The pharmacologically active component of CRLX101—CPT—has intrinsic fluorescence (Excitation$_{max}$ = 370 nm and Emission$_{max}$ = 435 nm), and can be used for the detection of CRLX101 in tissue via fluorescence microscopy (5, 6, 8). Fig. 2*A* illustrates detection of CPT fluorescence in two different types of human tumor xenografts in mice 24 h after i.v. dosing of CRLX101. The fluorescence signal has a patchy distribution throughout the tumor with some areas of densely clustered punctate fluorescence signal, whereas other areas are devoid of signal.

Fig. 2 *B* and *C* illustrates detection of CPT fluorescence in human gastric tumor biopsy specimens. The CPT signal observed was qualitatively similar to that obtained from the xenograft tumors (examples of CPT signal observed in other patients are shown in *SI Appendix*, Fig. S1). Distribution of CPT fluorescence was focal and punctate. To verify that observed signal was indeed CPT, regions of interest were repeatedly scanned using the confocal laser. CPT is a weak fluorophore and rapidly photobleaches upon repeated interrogation, compared with nonspecific tissue autofluorescence. Thus, punctate fluorescence that rapidly diminished upon multiple scans was determined to be from CPT (*SI Appendix*, Fig. S2). In total, CPT fluorescence was detected in all nine posttreatment tumors. No definitive CPT fluorescent signal was observed in any of the adjacent nontumor biopsy specimens (Table 1). One patient showed potential CPT signal in the posttreatment nontumor tissue biopsy; however, this

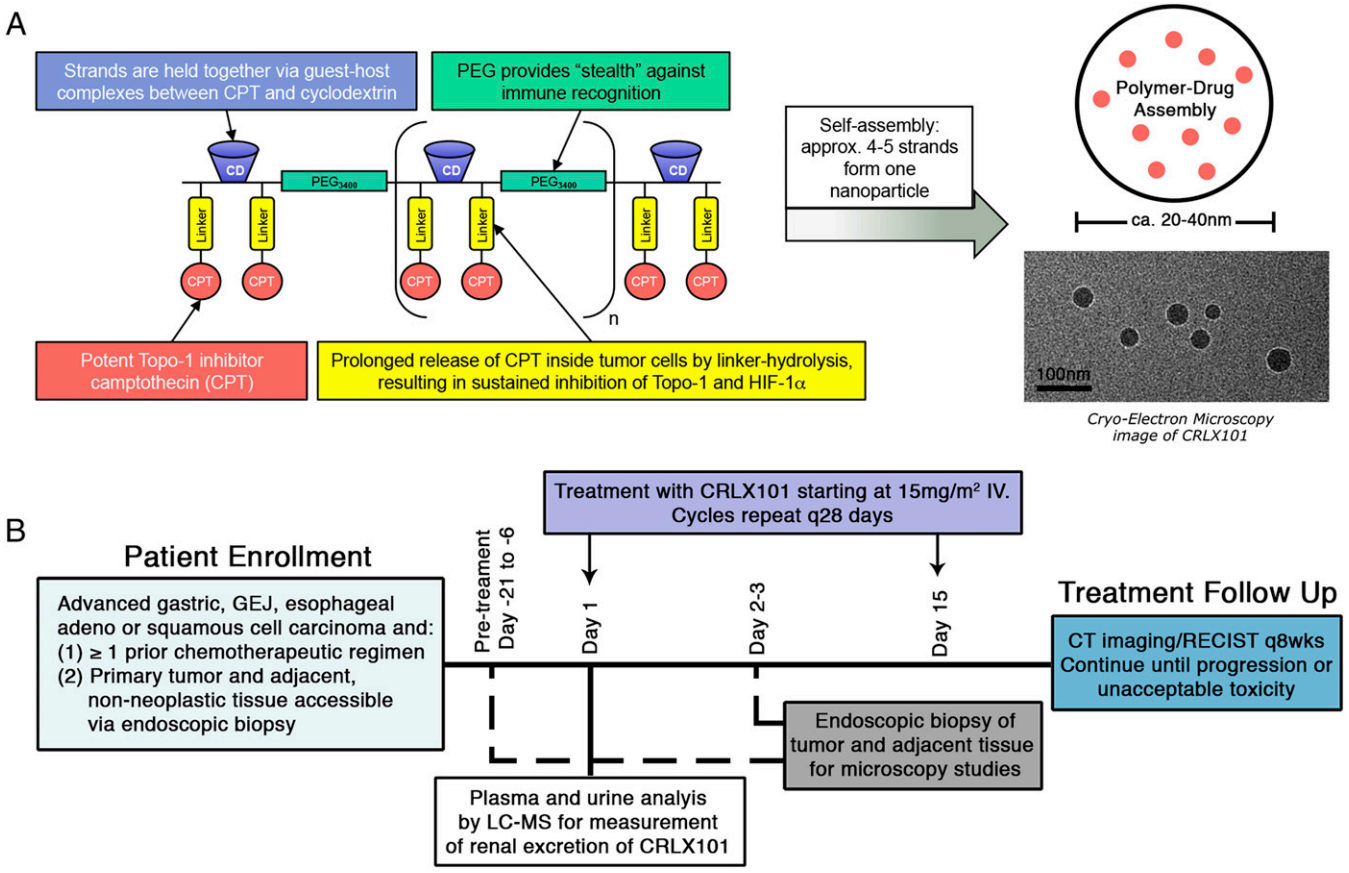

Fig. 1. Schematic of CRLX101 and study design. (*A*) CRLX101 nanoparticle design and particle formation including image of particles under cryoelectron microscopy. (*B*) Design of clinical trial.

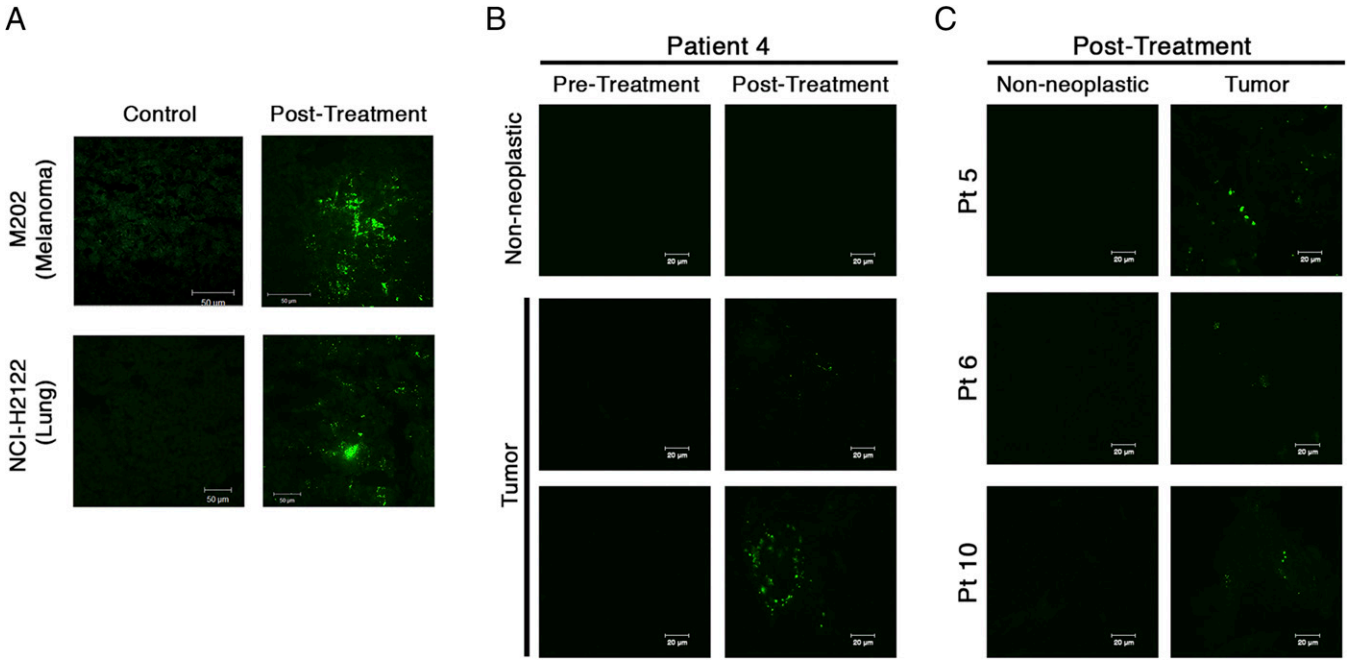

Fig. 2. Detection of camptothecin (CPT) fluorescence following CRLX101 treatment in mice and humans. (*A*) Presence of CPT in mice bearing two different human tumor xenografts. CPT is apparent 24 h after a single CRLX101 dose and appears as bright, punctate dots (green dots) with a patchy distribution throughout the tissue. (*B*) CPT signal in nonneoplastic and tumor tissue of a single patient under different dosing states. Positive CPT signal (green dots) is seen only in the posttreatment tumor tissue. (*C*) CPT signal in posttreatment nonneoplastic and tumor tissue for three other patients.

signal did not fully quench from repeated laser scans, thereby not meeting our criteria for definitive CPT signal (*SI Appendix*, Fig. S3). Fluorescence was considerably rarer in the patient samples than in the xenograft tumors. However, the patient biopsies were only a fraction of the size of pieces of xenograft tumor that we investigated. Tissue samples were also stained with an antibody against the PEG component of CRLX101 (Fig. 3). In five of nine patients, the PEG antibody colocalized with the CPT fluorescence, suggesting intact nanoparticles were present within the posttreatment tumors.

Pharmacodynamics Investigation of CRLX101 in Human Gastric Tumors. To confirm the pharmacokinetic observations, a pharmacodynamics study was performed. A hematoxylin and eosin (H&E) stain was performed first to verify the quality of existing tumors and surrounding, uninvolved tissue (*SI Appendix*, Fig. S4). The carbonic anhydrase IX (CA IX) antibody stain showed high intracellular expression in pretreated tumor samples, whereas the posttreatment samples revealed much less staining, suggesting a decrease in HIF-1α, a transcription factor upstream of CA IX (9) (Fig. 4*A*). The topoisomerase I (Topo-I) stain showed reduced staining from pretreatment to posttreatment samples (Fig. 4*B*). This result suggests CPT, released from the nanoparticle, bound Topo-I and triggered its degradation.

Discussion

The ability of intact nanoparticles to extravasate and deposit within tumor tissue is fundamental to their therapeutic activity

Table 1. Summary of biopsy investigation results for each patient

Patient	Tumor differentiation	Pretreatment nonneoplastic tissue	Pretreatment tumor tissue	Posttreatment nonneoplastic tissue	Posttreatment tumor tissue
2	Poor	0	0	0	++
3	Well	0	0	0	++*
4	Moderate to poor	0	0	0	+++*
5	Moderate	0	0	0	++*
6	Poor	0	0	0	++*
7	Poor	0	0	0	++
8	Moderate	0	0	+	++*
9	Moderate to poor	0	0	0	++
10	Poor	0	0	0	++

Tumor quality was determined using standard histological techniques. CPT signal in the tissue sample was graded in the following ways: 0 indicates no CPT signal was observed in the tissue; + indicates potential CPT signal was observed in the tissue, but did not meet both requirements used to determine true CPT signal [(*i*) observed signal was punctate and patchy in distribution and (*ii*) signal rapidly diminished upon repeated confocal laser scans]; ++ indicates definitive CPT signal was observed but only in a minority of images acquired; and +++ indicates definitive signal was observed in the majority of images acquired. Tissues marked by an * indicate CPT signal colocalization with PEG stain was observed. Patient 1 was not included in the analysis because no tumor tissue was identified in the biopsy samples both pre and post-CRLX101 treatment.

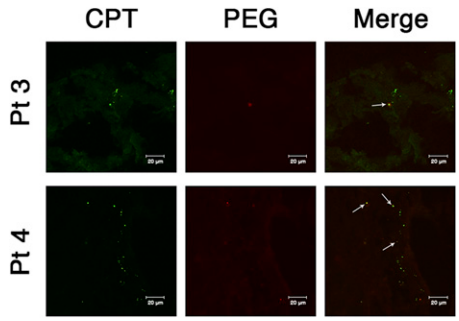

Fig. 3. CPT–PEG colocalization. Tissue samples were stained with an anti-PEG antibody to identify the polymer component of CRLX101. Evidence of colocalized CPT signal (bright green dots) and PEG stain (red dots) were observed in five of nine patients. White arrows indicate points of stain colocalization.

and selectivity. This mechanism of tumor deposition, known as the EPR effect, has only ever been demonstrated directly in animal models, specifically in xenograft tumors in mice that, in general, do not faithfully represent the true architecture of human tumors. There is considerable debate in the literature surrounding the existence of this phenomenon in human tumors. Because most nanoparticle therapeutics have been designed from the optimization of delivery to xenografted human tumors in mice, it is important to show that similar mechanisms of deposition take place in human tumors.

Here, we demonstrate through matched sets of pre- and postnanoparticle dosing biopsies of tumor and adjacent, nonneoplastic tissue evidence of intact nanoparticle deposition in human tumors after i.v. administration. All nine tumor-bearing patients showed evidence of CPT in the posttreatment tumor tissue. Furthermore, no definitive CPT signal was observed in adjacent, nonneoplastic tissue. Interestingly, the signal observed within the human tumors appeared to be solely due to drug within the tumor parenchyma. If drug were retained within the microvasculature following tissue fixation and processing, we would expect to see some signal in the normal tissue, but this was not observed. Due to poorly preserved tissue architecture of the fresh-frozen biopsy samples following processing, identification of drug signal within different tumor compartments (e.g., intracellular vs. interstitial) was not possible. An understanding of how uniformly and deeply CRLX101 diffuses throughout the tumor and how this affects free drug concentration within the tumor is critical to maximizing CRLX101 efficacy.

Although there was detectable CPT signal in the posttreatment tumors, it was significantly lower than what we have previously experienced in mouse xenografts (Fig. 2). CRLX101 first enters mouse model xenografts within 6 h of i.v. administration and slowly diffuses away from blood vessels and deeper into tumors over several days (5). Therefore, the quantity of CPT present in the patient samples 24 h after treatment may strongly depend on location of the biopsy relative to vasculature. The biopsies were acquired randomly from a patient's primary tumor and measured only ~3 mm^3, which is just a fraction of the total tumor volume. In contrast, it is possible to isolate entire xenografts and readily identify vasculature and areas of high drug signal. Human tumors also express a high degree of heterogeneity (10, 11). In patients with gastric cancer, the tumor microvascular density can significantly vary depending on the extent of invasion to surrounding tissues as well as gross tumor morphology (12). Factors that influence vascular density and heterogeneity within human tumors may affect the magnitude and reproducibility of the EPR effect in humans.

To investigate whether intact nanoparticles were present within the human tumors, an antibody against the PEG component of CRLX101 was used (Fig. 3). In five of nine patients, colocalization of the CPT signal with the PEG stain was observed, suggesting that at least some drug is still retained within intact nanoparticles in these tissues. In vitro investigation of CPT release from CRLX101 has shown only 30% of loaded CPT released from the nanoparticle at neutral pH after 24 h with that value dropping to 10% at the tumor microenvironment pH (pH 6.5–6.9) (13). These kinetics suggest a significant portion of the loaded CPT should be retained within the nanoparticle core when the posttreatment biopsies were acquired. Experiments using PET with radiolabeled CRLX101 in mice have shown increasing, selective accumulation of the nanoparticle within tumors over the first 24 h after an initial dose (8). A similar result was found using MRI where CRLX101 showed increasing apparent diffusion coefficient over the first 7 d after dosing in tumor-bearing mice (14). Both these in vivo results indicate intact nanoparticles are likely accumulating within the human tumors over the first 24–48 h. The lack of colocalized CRLX101 polymer-CPT signal in four of the nine patients may be explained by poor sensitivity of the anti-PEG antibody stain used. Several PEG mAbs were investigated and all showed significantly decreased affinity to the CRLX101 polymer component after exposure to tissue fixation agents. This likely limited the ability to detect the CRLX101 polymer within the fixed tissue sections. Combined with the scarcity of positive CPT signal in most tumor biopsies, this factor may have caused false negative colocalization results for the four patients. It is also possible that these patients experienced less overall nanoparticle deposition into the tumor due to tumor characteristics that are unfavorable—compared with the six positive patients—to nanoparticle extravasation, reducing potential binding sites for the PEG antibody.

Despite relatively low CPT signal in the human tumor compared with mouse xenograft tissue, investigation of tumor biomarkers showed clear pharmacodynamic effects of the drug within tumors. CA IX expression is driven directly by HIF-1α and can be used to measure HIF-1α activity. The decreased expression of CA IX in the posttreatment tumors is consistent with the inhibitor effect of CRLX101 on HIF-1α expression, which has been previously observed (7, 15). CPT has been known to cause rapid degradation of Topo-I through the ubiquitin–proteasome system in tissue culture (16–20). Our result reveals this may also be occurring in vivo as evident by the lower staining of Topo-I in the posttreatment tumors. This finding, to our knowledge, would be the first result demonstrating down-regulation of Topo-I by CPT in human tumors collected from clinical trials.

In summary, we show evidence of the nanoparticle CRLX101 accumulating within gastric tumors in humans but not adjacent, nonneoplastic tissue. This result supports the hypothesis that nanoparticle therapeutics can localize within human solid

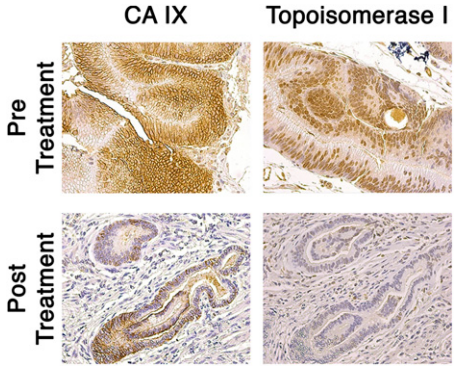

Fig. 4. Pharmacodynamics investigation of tumor biomarkers. Tumor tissues of six patients were stained for two different tumor biomarkers (CA IX and Topo-I) before and after treatment with CRLX101. The results shown here are indicative of the trend observed in the six individual tissue series.

tumors, and this may occur via the EPR effect. Colocalization of the CPT and PEG components of CRLX101 was observed in several patients, indicating intact nanoparticles are reaching tumors in humans. Although signal observed from the CPT component of CRLX101 was lower than what had been previously observed in xenografts, this decrease might be due to biopsy sampling location and tumor heterogeneity, and in particular, microvascular density. IHC revealed changes in two tumor biomarkers consistent with the biological activity of CPT within tumors.

Materials and Methods

Mice Studies. All mice were treated according to the National Institutes of Health Guidelines for Animal Care and Use (21) as approved by the Caltech Institutional Animal Care and Use Committee. Mice were treated with CRLX101 via lateral tail vein injection, then euthanized after 24 h. Their tumors were resected, embedded in optimal cutting temperature compound, and frozen for fluorescence microscopy.

Patient Enrollment and CRLX101 Treatment. Patients with advanced gastric, gastroesophageal junctional, esophageal adenocarcinoma carcinoma, or squamous cell carcinoma, who had progressed on at least one prior line of systemic therapy, were enrolled in a pilot clinical trial to assess preferential uptake of CRLX101 in tumor tissue versus healthy, adjacent tissue (ClinicalTrials.gov identifier: NCT01612546). All systemic therapy for patients was discontinued at least 4 wk before receiving CRLX101. Pretreatment biopsies were acquired by endoscopy 6–21 d before receiving the first i.v. infusion of 15 mg/m^2 CRLX101. The posttreatment biopsies were performed between 24 and 48 h after receiving CRLX101.

Human Gastric Tissue Sample Acquisition and Preparation. Human gastric tissue samples were obtained from patients enrolled in a CRLX101 pilot trial with consent in accordance with City of Hope Institutional Review Board (IRB) guidelines (City of Hope IRB Protocol 11276). Biopsy specimens used for fluorescence were immediately embedded in optimal cutting temperature media and frozen on dry ice. Biopsies acquired for IHC were immediately placed in 4% (wt/vol) paraformaldehyde. All specimens were transferred to the City of Hope Translational Research Laboratory before processing. The clinical trial was sponsored by the City of Hope. CRLX101 was supplied by Cerulean Pharma Inc.

Tissue Immunofluorescence. Fresh frozen tissue samples were sectioned, washed briefly in PBS, and fixed for 10 min with 10% formalin. Slides were blocked for 1 h in 5% (vol/vol) normal goat serum in PBS and followed by overnight stain at 4 °C with an anti-PEG antibody (1:100 dilution, Abcam ab94764). Slides were then washed and stained for 1 h with an Alexa Fluor 488-conjugated secondary antibody (1:500 dilution, Invitrogen A-21212) and mounted using ProLong Gold antifade reagent. Tissues were imaged with a Zeiss LSM 510 inverted confocal scanning microscope using a Zeiss Plan Neofluar 63×/1.25 oil objective. The excitation wavelength for camptothecin was 710 nm (two-photon laser) and 488 nm for detection of PEG. The corresponding emission filters were 390–465 nm and 565–615 nm, respectively. Images were adjusted to have equivalent mean brightness using the brightness adjustment tool in LSM 5 Image Browser (Leica).

Tumor Biomarker Immunohistochemistry. Tumor tissues were fixed with 10% formalin and embedded in paraffin. Tissues sections, 5 μm in thickness, were prepared and deparaffinized in xylenes followed by rehydration in graded alcohols. The sections were baked in 0.01 M sodium citrate buffer, pH 6.0, for 15 min for antigen retrieval. Endogenous peroxidase was quenched with 3% (vol/vol) hydrogen peroxide at room temperature (20–25 °C). Primary rabbit Topo-I (Santa Cruz) and rabbit CA IX (Proteintech) were applied overnight at 4 °C with final concentrations of 1:200 (Topo-1) and 1:2,000 (CA IX). The sections were counterstained with hematoxylin, followed by dehydration in graded alcohols and xylenes. Tissue sections were then developed using horseradish peroxidase DAB Quanto kit according to the manufacturer's instructions (Thermal Scientific). Sections containing no primary antibody stain were processed simultaneously and used as negative controls, whereas samples known to strongly express Topo-I and CA IX served as positive controls. Photomicrographs were taken on a Leica microscope equipped with a CCD camera (Leica Microsystems).

ACKNOWLEDGMENTS. We thank the patients and families who participated in this study. This work was supported by National Cancer Institute Grants CA 151819 and L30 CA179788-01, National Institutes of Health Grant 2K12CA001727-21, and by Cerulean Pharma Inc.

1. Davis ME, Chen ZG, Shin DM (2008) Nanoparticle therapeutics: An emerging treatment modality for cancer. *Nat Rev Drug Discov* 7(9):771–782.
2. Harrington KJ, et al. (2001) Effective targeting of solid tumors in patients with locally advanced cancers by radiolabeled pegylated liposomes. *Clin Cancer Res* 7(2):243–254.
3. Koukourakis MI, et al. (1999) Liposomal doxorubicin and conventionally fractionated radiotherapy in the treatment of locally advanced non-small-cell lung cancer and head and neck cancer. *J Clin Oncol* 17(11):3512–3521.
4. Davis ME, et al. (2010) Evidence of RNAi in humans from systemically administered siRNA via targeted nanoparticles. *Nature* 464(7291):1067–1070.
5. Eliasof S, et al. (2013) Correlating preclinical animal studies and human clinical trials of a multifunctional, polymeric nanoparticle. *Proc Natl Acad Sci USA* 110(37):15127–15132.
6. Weiss GJ, et al. (2013) First-in-human phase 1/2a trial of CRLX101, a cyclodextrin-containing polymer-camptothecin nanopharmaceutical in patients with advanced solid tumor malignancies. *Invest New Drugs* 31(4):986–1000.
7. Pham E, et al. (2015) Translational impact of nanoparticle-drug conjugate CRLX101 with or without bevacizumab in advanced ovarian cancer. *Clin Cancer Res* 21(4):808–818.
8. Schluep T, et al. (2009) Pharmacokinetics and tumor dynamics of the nanoparticle IT-101 from PET imaging and tumor histological measurements. *Proc Natl Acad Sci USA* 106(27):11394–11399.
9. Kaluz S, Kaluzová M, Liao S-Y, Lerman M, Stanbridge EJ (2009) Transcriptional control of the tumor- and hypoxia-marker carbonic anhydrase 9: A one transcription factor (HIF-1) show? *Biochim Biophys Acta* 1795(2):162–172.
10. Maeda H (2015) Toward a full understanding of the EPR effect in primary and metastatic tumors as well as issues related to its heterogeneity. *Adv Drug Deliv Rev* 91:3–6.
11. McGranahan N, Swanton C (2015) Biological and therapeutic impact of intratumor heterogeneity in cancer evolution. *Cancer Cell* 27(1):15–26.
12. Araya M, et al. (1997) Microvessel count predicts metastasis and prognosis in patients with gastric cancer. *J Surg Oncol* 65(4):232–236.
13. Cheng J, Khin KT, Jensen GS, Liu A, Davis ME (2003) Synthesis of linear, β-cyclodextrin-based polymers and their camptothecin conjugates. *Bioconjug Chem* 14(5):1007–1017.
14. Ng TSC, et al. (2013) Serial diffusion MRI to monitor and model treatment response of the targeted nanotherapy CRLX101. *Clin Cancer Res* 19(9):2518–2527.
15. Gaur S, et al. (2014) Pharmacodynamic and pharmacogenomic study of the nanoparticle conjugate of camptothecin CRLX101 for the treatment of cancer. *Nanomedicine (Lond)* 10(7):1477–1486.
16. Desai SD, Liu LF, Vazquez-Abad D, D'Arpa P (1997) Ubiquitin-dependent destruction of topoisomerase I is stimulated by the antitumor drug camptothecin. *J Biol Chem* 272(39):24159–24164.
17. Fu Q, Kim SW, Chen HX, Grill S, Cheng YC (1999) Degradation of topoisomerase I induced by topoisomerase I inhibitors is dependent on inhibitor structure but independent of cell death. *Mol Pharmacol* 55(4):677–683.
18. Lin C-P, Ban Y, Lyu YL, Liu LF (2009) Proteasome-dependent processing of topoisomerase I-DNA adducts into DNA double strand breaks at arrested replication forks. *J Biol Chem* 284(41):28084–28092.
19. Zhang H-F, et al. (2004) Cullin 3 promotes proteasomal degradation of the topoisomerase I-DNA covalent complex. *Cancer Res* 64(3):1114–1121.
20. Desai SD, et al. (2003) Transcription-dependent degradation of topoisomerase I-DNA covalent complexes. *Mol Cell Biol* 23(7):2341–2350.
21. Committee on Care and Use of Laboratory Animals (1996) *Guide for the Care and Use of Laboratory Animals* (Natl Inst Health, Bethesda), DHHS Publ No (NIH) 85–23.